Numerical Dosimetric Investigation of a Wireless Charger

Report

Quotation #5200354-C to Molex CVS Dabendorf GmbH

Document Version 1.0 / 24th August 2020

Authors: David Schäfer, Winfried Simon

IMST GmbH
Carl-Friedrich-Gauß-Str. 2–4
47475 Kamp-Lintfort
Germany

Information

File Name	Report_WCH-302_V1.0.pdf
Initial Date	24th August 2020
Page count	17

Versions

Release Date	Version	Author	Comments
24th August 2020	1.0	David Schäfer	Initial version

Approval

Name	Job Title	Date	Signature
David Schäfer	Project leader	24th August 2020	
Winfried Simon	Team leader "EM Modeling"	24th August 2020	

Device Under Test (DUT)

Type of DUT:	Wireless Power Charger
Model Name:	WCH-302
FCC ID:	RK7WCH-302
Frequency band:	127.55 kHz
Antenna:	Two integrated loop coils
Applicant:	Molex CVS Dabendorf GmbH Märkische Strasse 72, 15806 Zossen OT Dabendorf, Germany Contact: Ines Baufeld

Human Exposure Limits (47 C.F.R. § 2.1093)

Condition	Uncontrolled Environment (General Population)		Controlled Environment (Occupational)	
	SAR Limit	Mass Avg.	SAR Limit	Mass Avg.
SAR averaged over the whole body mass	0.08 W/kg	whole body	0.4 W/kg	whole body
Peak spatially-averaged SAR for the head, neck & trunk	1.6 W/kg	1 g of tissue*	8 W/kg	1 g of tissue*
Peak spatially-averaged SAR in the hands, wrists, feet and ankles	4.0 W/kg	10 g of tissue*	20 W/kg	10 g of tissue*
Note: *Defined as a tissue volume in the shape of a cube				

Evaluation Result

$SAR_{1g, max}$ in forearm phantom	Below the 47 C.F.R. § 2.1093 limit?
11.88 mW/kg = 0.01188 W/kg	Yes

Contents

List of Figures

List of Tables

1 Introduction

1.1 Objective

The objective of the investigation is the numerical dosimetric assessment of a wireless charger (further referred to as “device under test” or “DUT”) for portable devices (further referred to as ”receiver device”) like e.g. smartphones. Technical data of the DUT necessary for creating the numerical model, the validation of the model as well as the specification of the human body model configuration were contributed by Molex (further referred to as ”applicant”).

1.2 Simulation Method

All simulations were done with the Finite Difference Time Domain (FDTD) simulation tool Empire XPU [1]. A numerical model of the DUT was generated and validated by measurements of the magnetic field in its vicinity. The spatially averaged (1g cubes) Specific Absorption Rate (SAR) in a human body part model (phantom) was investigated similar to the assessment procedures described in IEC/IEEE 62704-1 [2, 3].

1.3 DUT Description

The applicants 15 W, dual coil, wireless power charger ”WCH-302” is developed for automotive applications. The mechanical assembly of the product is depicted in Figure 1. During operation only one of the two coils is excited/charging at a time. Which coil is used for charging is chosen by the DUT depending on the placement of the receiver device.

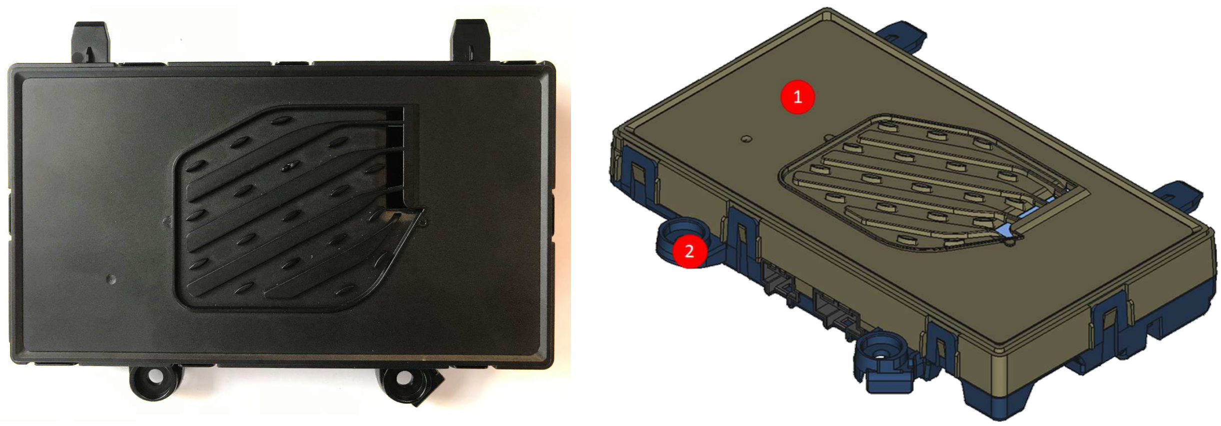

(a) (b)

Figure 1: (a) Photo and (b) CAD image of the DUT with (1) the upper and (2) the lower part of the dielectric housing.

The DUT can be installed in different configurations. The worst-case installation location is expected to be the vehicles rear-seat arm-rest, where it is possible for the passenger to place his arm on the DUT during the operation of charging.

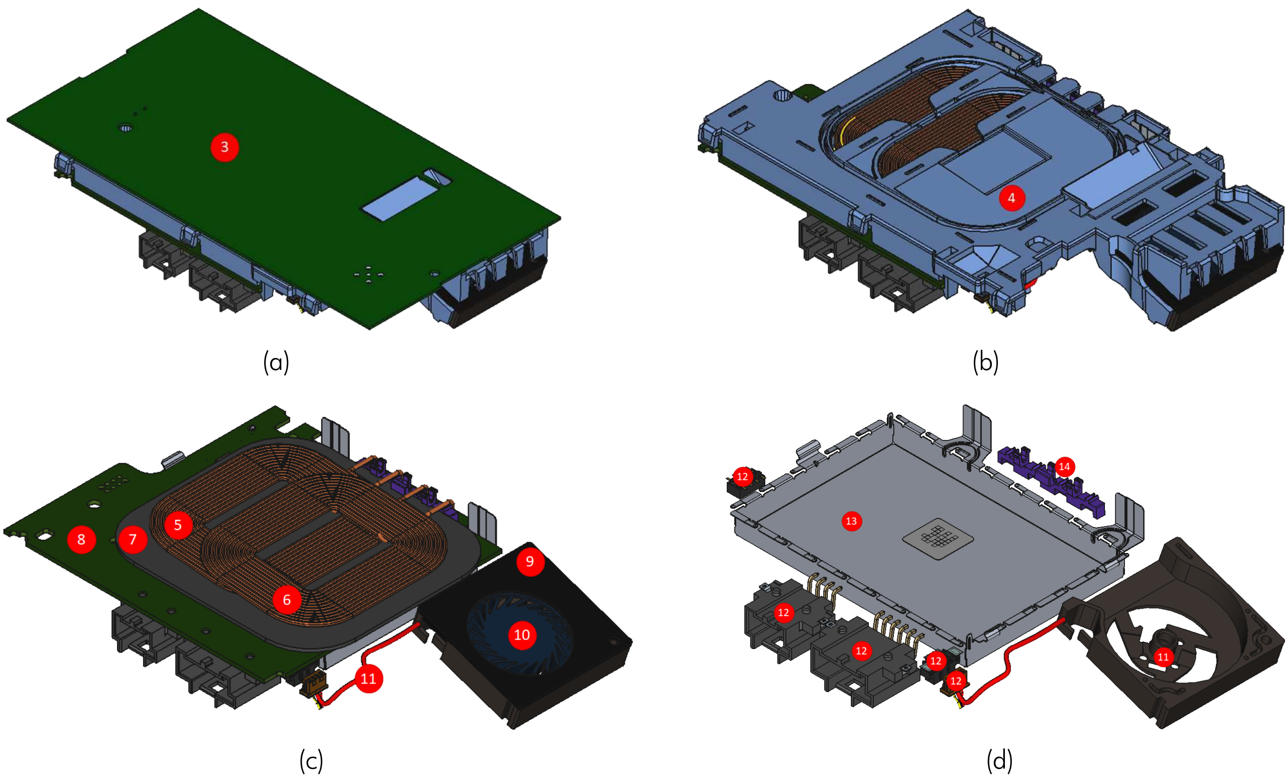

Figure 2: DUTs mechanical stack up with: (3) antenna PCB, (4) dielectric support structure, (5) wireless charging coil 0, (6) wireless charging coil 1, (7) ferrite, (8) main PCB, (9-11) fan with fan-housing and cable, (12) connectors, (13) shielding cover, (14) dielectric support structure.

1.4 Measurement Setup for Validation

A validation of the EM model was carried out by comparing the simulated and measured magnetic field in the vicinity of the DUT. Due to the applicants internal assessment the worst-case configuration is given when coil 0 is excited, so this operation state was considered. The magnetic field levels were measured at the applicants internal laboratory with the setup depicted in Figure 3.

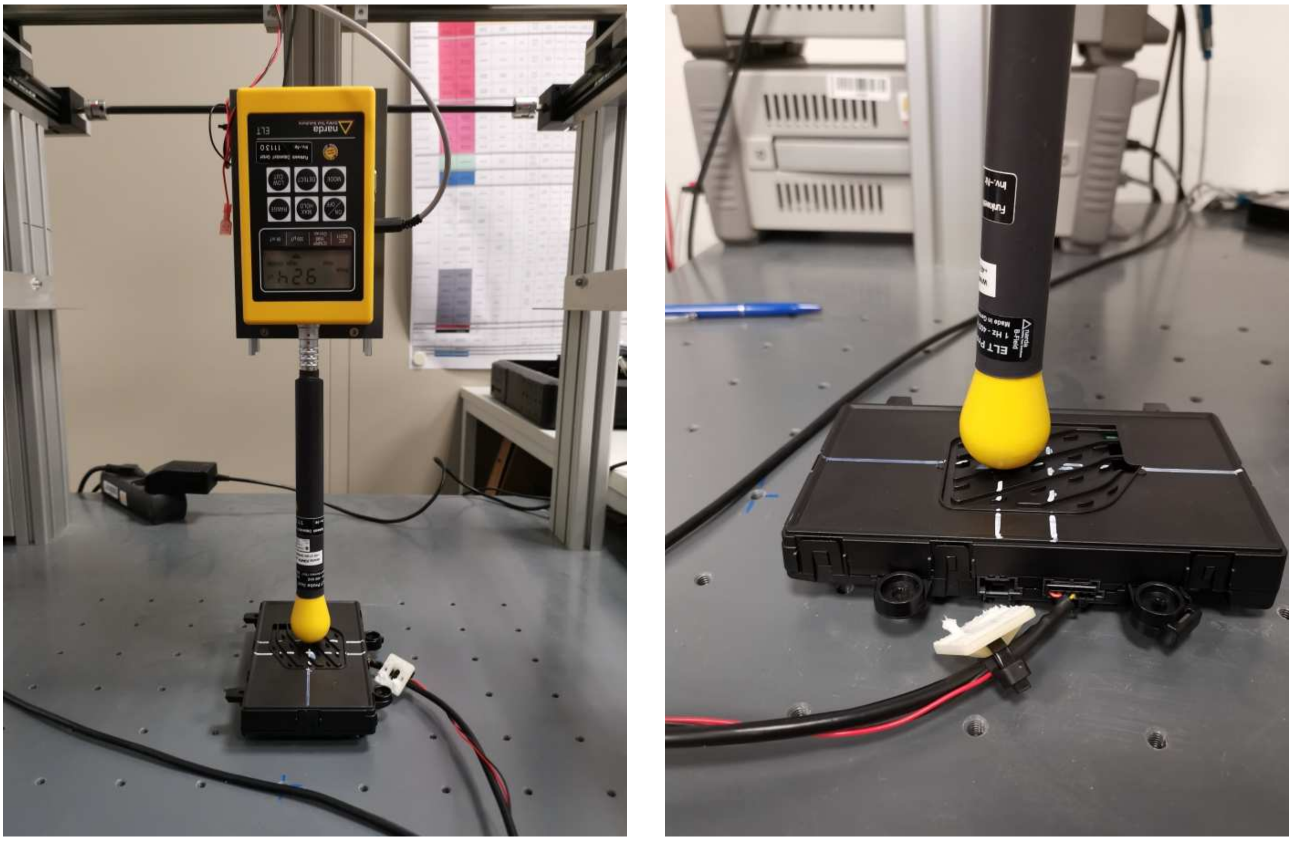

(a) (b)

Figure 3: Measurements setup. The crossings of the white lines indicate the xy-center of the two coils. The pictures show the lowest possible position of the field probe (touching the DUTs housing).

The measurements were executed with a "Narda ELT-400" magnetic field meter and a $3\,\text{cm}^2$ magnetic field probe. A series production DUT was used, running in a testing operating mode without receiver device at the maximum expectable coil current of 3.47 A RMS. The field probe was located directly above the xy-center of coil 0, which is indicated by the crossings of the white lines in Figure 3. A line measurement of the magnetic flux density was performed by lifting the probe upwards to different z-distances from the DUT. The pictures show the lowest possible position of the field probe.

2 EM Simulation Model

2.1 Model Setup

The simulation model is based on STEP CAD data and ODB++/Gerber layout data provided by the applicant. The data was imported into Empire, whereby the coordinate origin of the STEP file was maintained. Figures 4 and 5 show 3D views of the simulation model, which consists of the following parts (top to bottom):

1. Antenna PCB, FR4 with copper traces ($\sigma = 58.13e6$ S/m)
2. Coil 0, copper (orange, $\sigma = 58.13e6$ S/m)
3. Coil 1, copper (green, $\sigma = 58.13e6$ S/m)
4. Ferrite, MnZn (gray, $\mu_r = 2300$, $tan(\delta) = 0.02076$)
5. Main PCB, FR4 with copper traces ($\sigma = 58.13e6$ S/m)
6. Shielding cover, steel ERGSTE-1.4310 (blue, $\sigma = 1.37e6$ S/m)

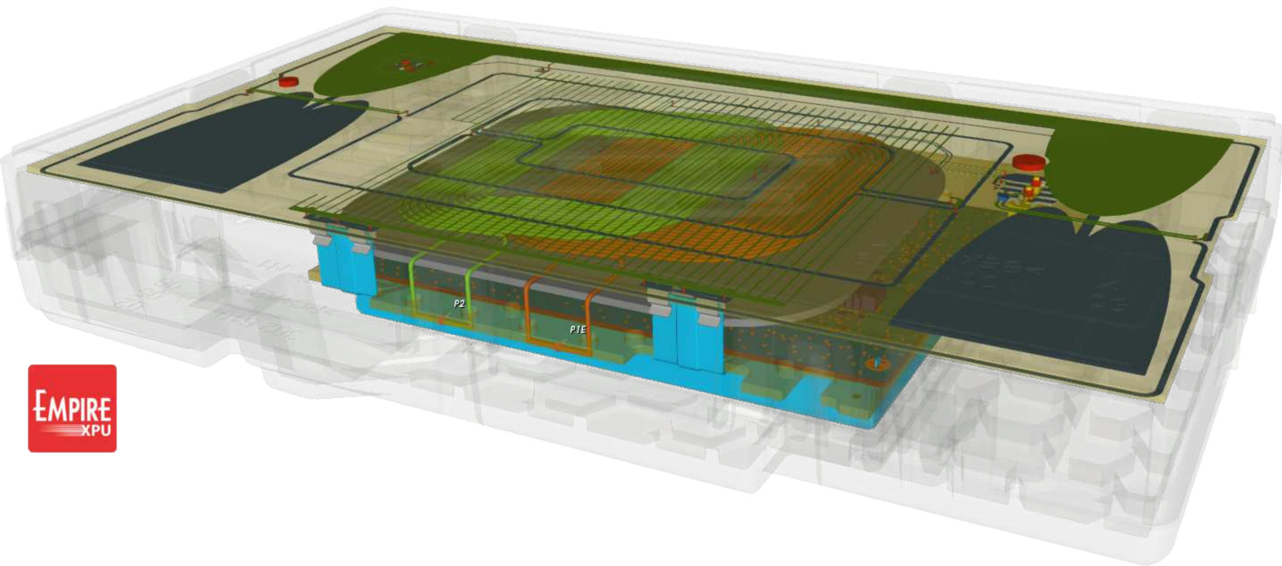

Figure 4: Geometry of the Empire simulation model of the DUT as overview.

The charging coil 0 (orange) can be seen beneath the substrate of the antenna PCB. The coils middle point is located at $x = 0$ mm and $y = -8.5$ mm and the top side of the housing is at $z = 24.6$ mm (outer housings rim is at $z = 25$ mm). The geometry of the DUTs dielectric housing is included in the model, but not considered in the EM simulation (no material assigned).

2.2 Model Validation

The simulation model was validated by comparing the simulated and measured magnetic fields (cf. section 1.4). During measurement coil 0 was excited with a current of 3.47 A (RMS) at a frequency of 127.55 kHz. Coil 1 was inactive, and for the simulation its input was terminated with a second non-excited port. As shown in Figure 3, the validation setup didn't include a receiver device or body model.

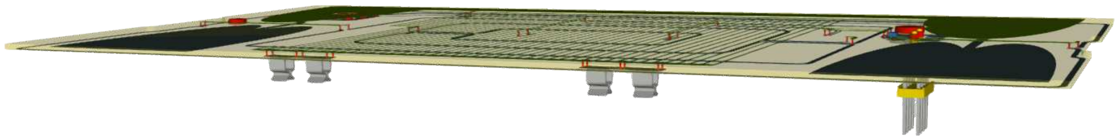

(a)

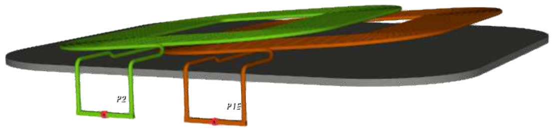

(b)

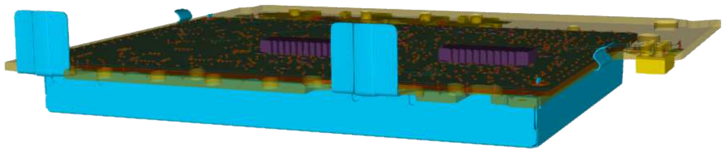

(c)

Figure 5: Exploded view of the simulation model: (a) Antenna PCB (b) Coil 0 (orange), coil 1 (green), ferrite (gray) and Empire ports (c) Main PCB and shielding cover (blue)

Figure 6 shows a xz-cutplane for the simulated magnetic field strength through the center ($x = 0$) of the DUT. It can be seen how shielding cover, main PCBs and ferrite confine the main part of the magnetic field to the dedicated receiver device location above the DUT.

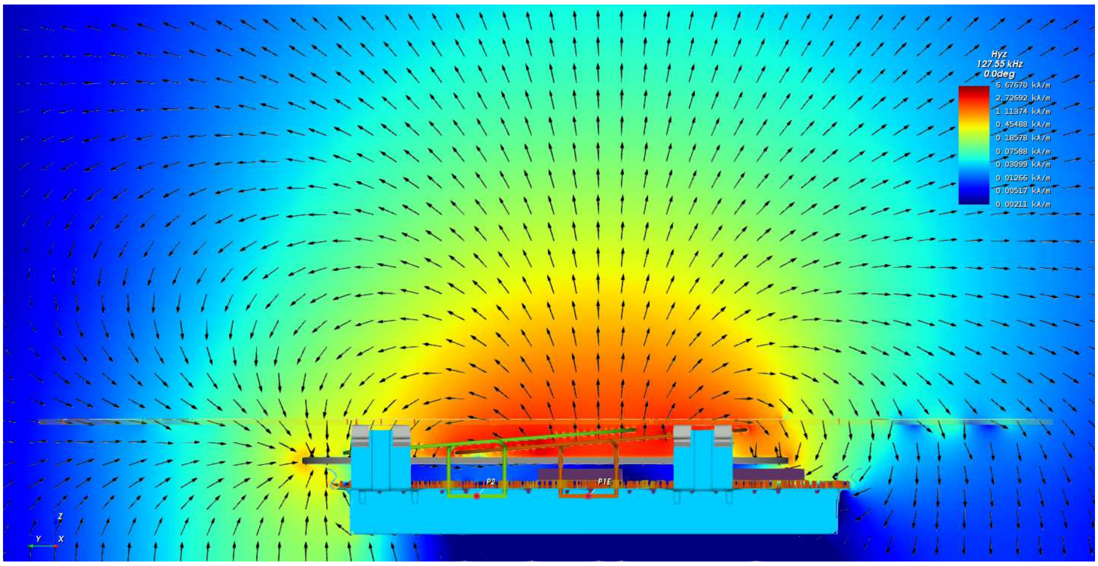

Figure 6: The simulated magnetic field displayed on a yz-plane through the DUT, calculated for a frequency of 127.55 kHz and a current of 3.7 A (RMS) through coil 0.

Analogue to the setup of the measurement (cf. section 1.4) the simulated magnetic field (H-field) strength was evaluated along a line in z-direction perpendicular to the top side of the DUTs housing, as can be seen in Figure 7. The line goes through the center of coil 0.

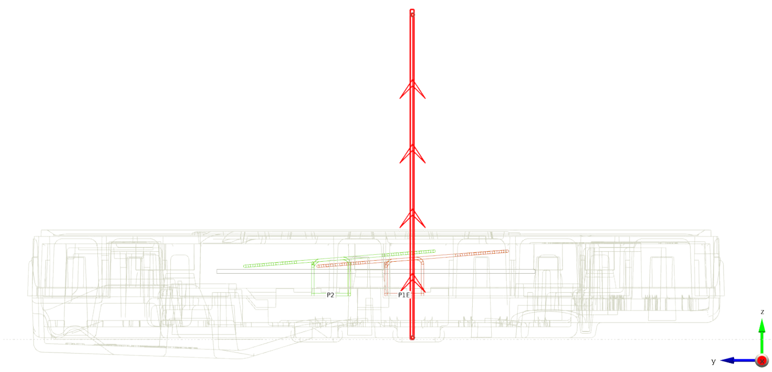

Figure 7: 2D side view (yz-plane) of the numerical model showing the line (red) along which the H-field is evaluated. The line is going through the center of coil 0.

Figure 8 shows the Empire simulation results compared to the measurements. Overall the figure shows a good fit in curve slope and behaviour. To achieve a better matching of the absolute field values, the simulated coil current was increased from 3.47 A (RMS) to 3.7 A (RMS). Assuming that the z-reference of the field probe is located 15 mm away from its tip, the simulated curve is in good agreement with the measurement.

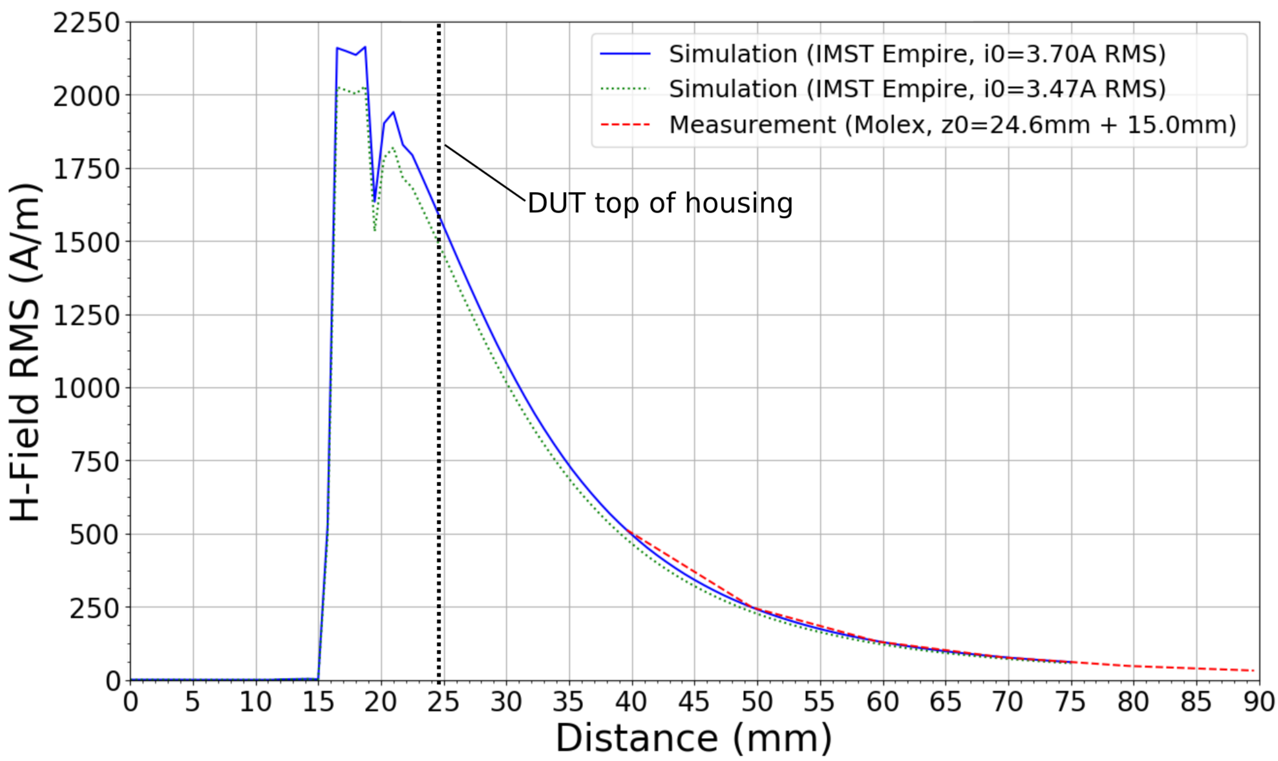

Figure 8: Curves for the line evaluation of the H-field. For an adapted coil 0 current of 3.7 A (RMS) the simulated curve is in good agreement with the measurement.

3 SAR Evaluation

For the evaluation of the Specific Absorbtion Rate (SAR) a human forearm phantom was added to the simulation model as shown in Figure 9. The phantom model is inhomogeneous and consists of anatomically correctly distributed tissue materials (skin, fat, muscle, bones, etc.). The tissues are modelled with gabriel materials (cf. table 4) and resolved with cube voxels of 0.5 mm edge length.

(a)

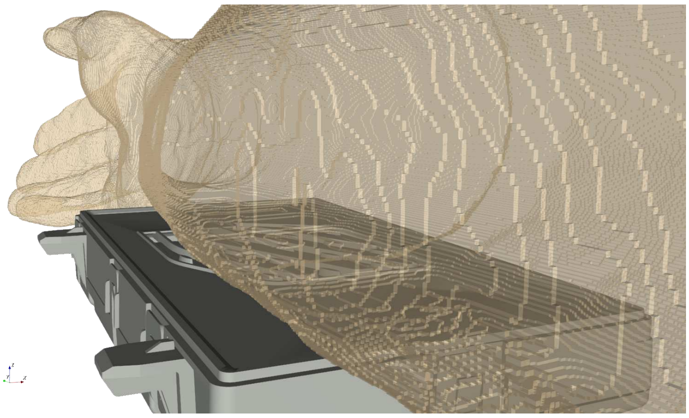

(b)

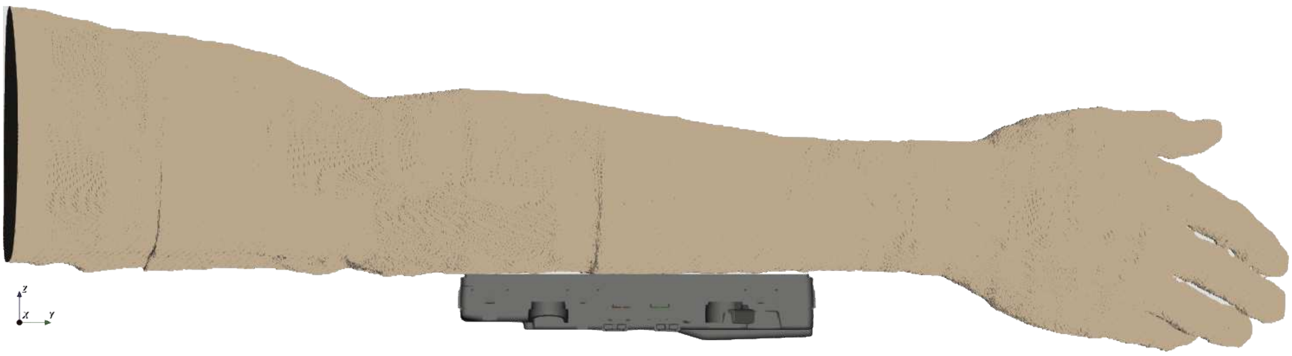

(c)

Figure 9: Geometry of the forearm phantom from different views.

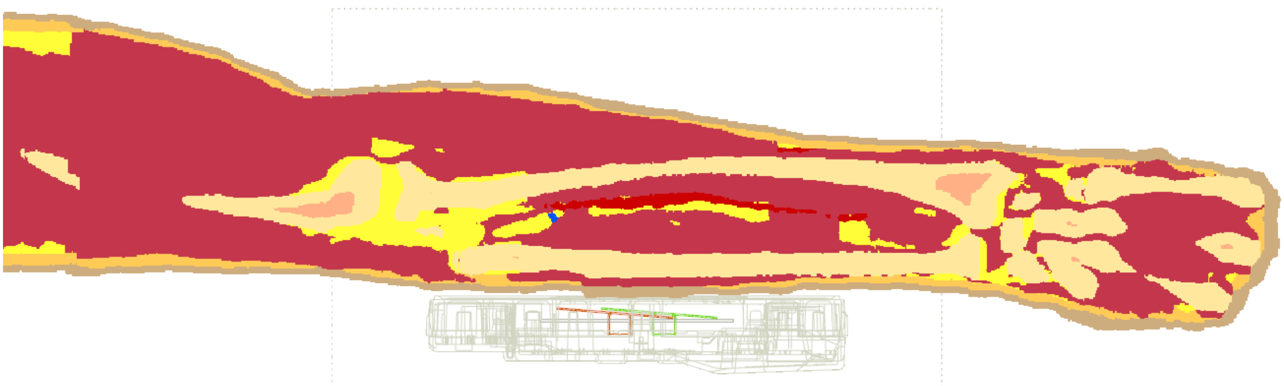

Figure 10: Material distribution inside the forearm phantom in a yz-cutplane.

Type and location of the phantom were specified by the applicant, considering the scenario of the DUT being installed into the rear-seat arm-rest of a vehicle (cf. section 1.3). The medial side of the forearm phantom is touching (contact area) the top of the DUTs housing directly above the charging coils. This setup assumes a worst-case malfunction scenario, where the DUT excites the coil without a receiver device being present. According to the applicant, the DUTs electronics take precautions to prevent this type of malfunction. During normal operation the receiver device is anticipated to partially shield the human body part from the magnetic field, thus decreasing the exposure.

3.1 Simulation Results

Figure 11 and 12 show the simulated 1g-averaged SAR as xy-cutplane and yz-cutplane, whereby the planes were moved to the position of the maximum. The maximum value for the simulated 1g-averaged SAR inside the phantom is 11.88 mW/kg at the position $x = -24.73$ mm, $y = -8.98$ mm, $z = 30.74$ mm.

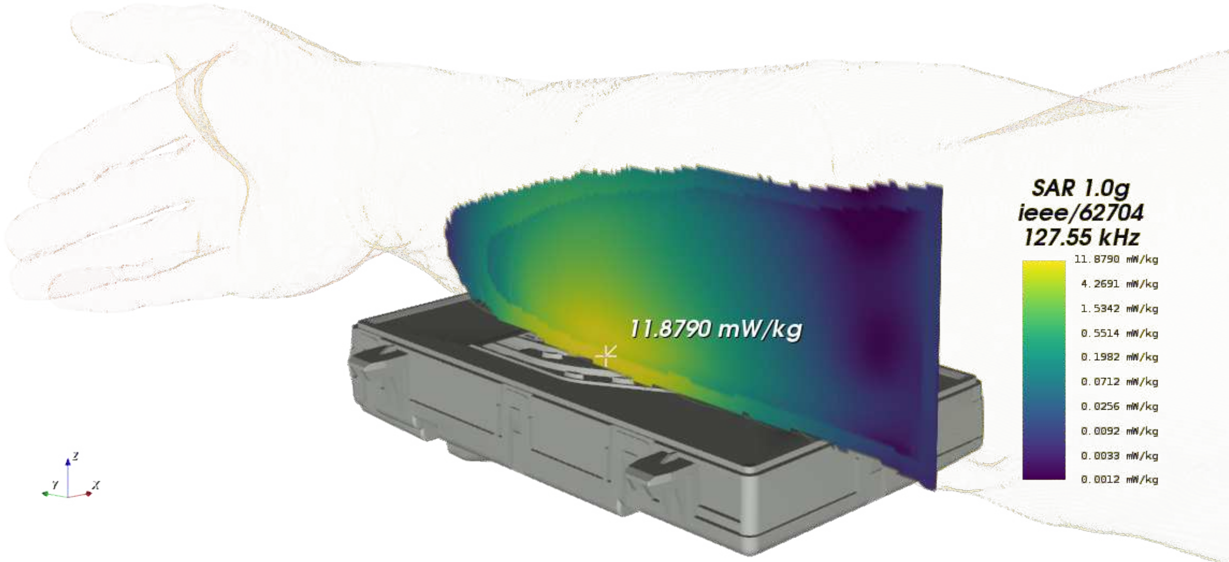

Figure 11: Simulated 1g-averaged SAR results shown as yz-cutplane. The plane is located at $x = -24.73$ mm which is the position of the maximum.

The discontinuities of the SAR near the surface of the phantom (cf. Figure 12) are caused by the special averaging algorithm applied to boundary areas, as required by IEC/IEEE 62704-1 [2].

3.2 Tolerance Analysis

To analyse the accuracy of the results for the numerical model presented in section 3.1 (further referred to as "reported model"), several variants were created and simulated. The coil current was fixed to 3.7 A (RMS) throughout the tolerance analysis.

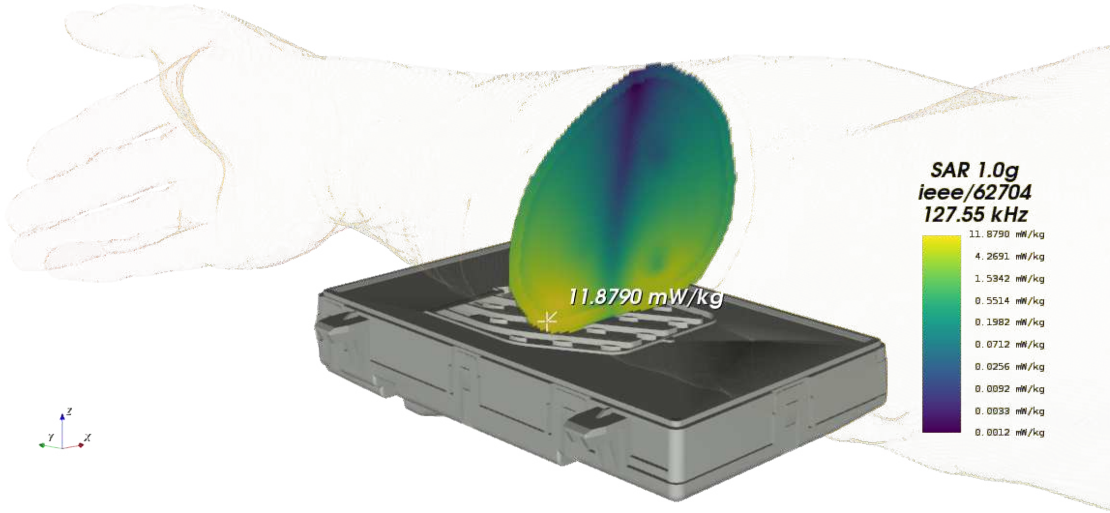

Figure 12: Simulated 1g-averaged SAR results shown as xz-cutplane. The plane is located at $y = -8.98$ mm which is the position of the maximum.

Domain Size	$220x234x146$ mm	$280x294x206$ mm
$\text{SAR}_{1\text{g, max}}$	11.88 mW/kg	11.58 mW/kg
Deviation	$0\,\%$	$-2.53\,\%$

Table 1: SAR results for different simulation domain sizes. The first data column corresponds to the reported model (cf. section 3.1). The simulation domain was enlarged symmetrically in all spatial directions.

Time/Convergence	15 Msteps	43 Msteps
Energy Decay	-92.20 dB	-93.06 dB
$\text{SAR}_{1\text{g, max}}$	11.88 mW/kg	12.06 mW/kg
Deviation	$0\,\%$	$+1.52\,\%$

Table 2: SAR results for different number of total time steps. The first data column corresponds to the reported model (cf. section 3.1).

Mesh Resolution	33.5 MCells	100.6 MCells
Timesteps	15 Msteps	30 Msteps
$\text{SAR}_{1\text{g, max}}$	11.88 mW/kg	12.53 mW/kg
Deviation	$0\,\%$	$+5.47\,\%$

Table 3: SAR results for different mesh resolutions. The first data column corresponds to the reported model (cf. section 3.1). In the area of the maximum SAR the cell size was divided by 8 (x, y, z-mesh halved). To compensate for the smaller FDTD timestep the simulation time was increased to 30 Msteps.

Table 1, 2 and 3 show the maximum SAR for the investigated variants as well as their relative deviation from the reported model. It can be seen, that none of the variants shows more than $5.5\,\%$ discrepancy for the SAR.

3.3 Conclusion

Summarizing the numerical dosimetric investigation of the DUT, the following can be stated:

1. The simulated magnetic field strength is in good agreement with the measurements (cf. section 2.2), indicating the accurate setup of the DUTs simulation model (without phantom).
2. The investigated scenario follows the worst-case assumption that:
   (a) The forearm phantom is in direct contact with the DUT.
   (b) The DUT is exciting coil 0 with the maximum expectable current, despite the fact that no receiver device is present (malfunction).
3. The determined maximum 1g-averaged SAR is 11.88 mW/kg. This corrsponds to $0.74\,\%$ of the allowed 1.6 W/kg SAR for localised exposure with devices used by the general public according to 47 C.F.R. § 2.1093 [4]. Given the choice of phantom configuration, the application of the higher exceptional 10g-averaged SAR limit of 4 W/kg for hands, wrists, feet and ankles exposure may be justified as well.
4. The tolerance analysis (cf. section 3.2) shows less than $5.5\,\%$ SAR deviation between variants and reported model, indicating that the simulation results for the DUT with phantom are accurate.
5. Considering the previous statements, the conclusion of this report is that the DUT does not exceed the SAR limits of 47 C.F.R. § 2.1093 [4].

4 Appendix

4.1 Specific Information for SAR Computational Modelling

Computational resources Computation was performed on a AMD Threadripper 3970x with 4.482 GB memory usage.

FDTD algorithm implementation and validation cf. [3]

Computing peak SAR from field components cf. [3]

1g-averaged SAR procedures cf. [2, 3]

Total computational uncertainty cf. [3] and section 3.2

Computational parameters:

- **Cell Size (min/max):** 0.15 mm / 1 mm
- **Domain Size:** $220x234x146$ mm
- **Total amount of mesh cells:** approx. 33.5 million
- **Time step:** 1.23521e-13 s
- **Total number of time steps:** approx. 15 million
- **Simulation time:** approx. 9 hours at 15000 million cells per second (15 GCells/s).
- **Excitation method:** Gaussian pulse with $f_0 = 0$ Hz, $f_{\text{BW}} = 50$ MHz

Phantom model implementation cf. section 3

Tissue dielectric parameters cf. table 4

Transmitter model implementation and validation cf. section 2

Test device positioning cf. section 3

Steady state termination procedures A Gaussian pulse was used for the excitation and the simulation was terminated when the energy has dissipated to more than 15 million time steps.

Test results for determining SAR compliance cf. section 3

4.2 Gabriel Material Properties

Tissue	Rel. Permittivity	Conductivity (S/m)	Amount (%)
Air External	1.000e+00	0.000e+00	86.399
Artery	5.071e+03	7.046e-01	0.048
Bone	2.184e+02	2.087e-02	0.783
Fat	8.910e+01	4.345e-02	0.699
Marrow red	1.570e+02	1.030e-01	0.041
Muscle	7.502e+03	3.677e-01	8.486
SAT (subc. fat)	8.910e+01	4.345e-02	1.389
Skin	1.115e+03	5.868e-04	2.102
Vein	5.071e+03	7.046e-01	0.054

Table 4: Gabriel material properties at 127.55 kHz for tissues included in the forearm phantom.

4.3 Abbreviations

Abbreviation	Description
CAD	Computer Aided Design
DUT	Device Under Test
EM	Electro Magnetic
FDTD	Finite Difference Time Domain
PCB	Printed Circuit Board
RF	Radio Frequency
RMS	Root Mean Square
SAR	Specific Absorption Rate

Table 5: Abbreviations.

5 References

[1] IMST GmbH. (2020, August) Empire XPU, v8.01. Carl-Friedrich-Gauß-Str. 2-4, 47475 Kamp-Lintfort, Germany. [Online]. Available: http://empire.de

[2] "IEC/IEEE International Standard – Determining the peak spatial-average specific absorption rate (SAR) in the human body from wireless communications devices, 30 MHz to 6 GHz - Part 1: General requirements for using the finite-difference time-domain (FDTD) method for SAR calculations," *IEC/IEEE 62704-1:2017*, pp. 1–86, 2017.

[3] IMST GmbH, "EMPIRE XPU - Code Verification according to IEC/IEEE P62704-1."

[4] Federal Communications Commission, "FCC Limits for Specific Absorption Rate (SAR), 47 C.F.R. § 2.1093," 2012.